

# Ontogeny of myeloperoxidase (MPO) positive cells in flounder (*Paralichthys olivaceus*)

Qiuji Gan<sup>1</sup>, Heng Chi<sup>1,3\*</sup>, Chengcheng Liang<sup>1</sup>, Letao Zhang<sup>1</sup>, Roy Ambli Dalmo<sup>2</sup>,  
Xiuzhen Sheng<sup>1,3</sup>, Xiaoqian Tang<sup>1,3</sup>, Jing Xing<sup>1,3</sup>, Wenbin Zhan<sup>1,3</sup>

<sup>1</sup> Laboratory of Pathology and Immunology of Aquatic Animals, KLMME, Ocean University of China, Qingdao, China

<sup>2</sup> Norwegian College of Fishery Science, Faculty of Biosciences, Fisheries and Economics, UiT - the Arctic University of Norway. Tromsø, Norway

<sup>3</sup> Laboratory for Marine Fisheries Science and Food Production Processes, Qingdao National Laboratory for Marine Science and Technology, Qingdao, China

\*To whom correspondence should be addressed

Mailing address:

Heng Chi

5 Yushan Road

Qingdao 266003, China

Phone: 86-532-82032284

E-mail: [chiheng@ouc.edu.cn](mailto:chiheng@ouc.edu.cn)

1 **Abstract**

2 Neutrophils represent an important asset of innate immunity. Neutrophils express  
3 myeloperoxidase (MPO) which is a heme-containing peroxidase involved in microbial  
4 killing. In this study, by using real-time quantitative PCR and Western blot analysis, the  
5 flounder MPO (*PoMPO*) was observed to be highly expressed in the head kidney,  
6 followed by spleen, gill, and intestine during ontogeny – during developmental stages  
7 from larvae to adults. Furthermore, *PoMPO* positive cells were present in major  
8 immune organs of flounder at all developmental stages, and the number of neutrophils  
9 was generally higher as the fish grew to a juvenile stage. In addition, flow cytometry  
10 analysis revealed that the proportion of *PoMPO* positive cells relative to leukocytes, in  
11 the peritoneal cavity, head kidney, and peripheral blood of flounder juvenile stage was  
12 18.3%, 34.8 %, and 6.0%, respectively, which is similar to the adult stage in flounder  
13 as previously reported. The presence and tissue distribution of *PoMPO* during ontogeny  
14 suggests that *PoMPO* positive cells are indeed a player of the innate immunity at all  
15 developmental stages of flounder.

16

17 **Keywords: Ontogeny; Myeloperoxidase; Innate immunity; Fish**

18

## 19 **Introduction**

20 One of the main problems in the worldwide production of marine fish is the high  
21 mortality rate during larviculture (Rojo-Cebreros et al., 2018; Austin, 2006; Bergh,  
22 2000). Disease susceptibility may be due to an immature immune defense system at  
23 early stages. It has been shown the first feeding represents a milestone of organ  
24 development in gadoids, flatfishes and sparids, while a continuous differentiation  
25 during the larval stage and metamorphosis occurs (Falk-Petersen, 2005). For many fish  
26 species, the immune system is fully operational at the stage of first feeding (Martin and  
27 Król, 2017; Yúfera and Darias, 2007).

28 It is acknowledged that main lymphoid organs of the teleost are the head kidney, thymus,  
29 spleen, gill- and mucous-associated lymphoid tissues (GIALTs and MALTs) (Patel et  
30 al., 2009; Dalum et al., 2021) – both in larvae and developmental stages later on  
31 (Campoverde et al., 2019; Liang et al., 2022). During the early life stages, larvae have  
32 to rely solely on innate immune mechanisms and possibly maternal antibodies until they  
33 develop a functional adaptive immune system, which may take a few weeks to months  
34 (Saurabh and Sahoo, 2008). The cellular innate immunity is partly executed by  
35 phagocytic cells such as neutrophils and macrophages (Gasteiger et al., 2016; Hirayama  
36 et al., 2017; Lee et al., 2022). They are involved in antibacterial defenses, both by  
37 phagocytosis and by subsequent intracellular killing, as well as the release of  
38 extracellular traps (ETs) (Ellis, 1999; Malech et al., 2020; Sollberger et al., 2018).  
39 Myeloperoxidase (MPO), a highly cationic, heme-containing, and glycosylated enzyme  
40 is a major protein in azurophilic granules of neutrophils and is one of the key molecules

41 in immune response (Odobasic et al., 2016). In the phagosomes, MPO is involved in  
42 sustaining an alkaline milieu, which is optimal for the activity of serine proteases and  
43 other granule components to inactivate and kill microbes (Arnhold, 2020). In the  
44 presence of hydrogen peroxide and halides, MPO catalyzes the formation of reactive  
45 oxygen intermediates, which facilitates microbial killing by neutrophils (Aratani, 2018).  
46 MPO is also a key component in ETs capable of inhibiting the proliferation of bacteria,  
47 such as *Staphylococcus aureus* (Morales-Primo et al., 2022). In teleost, MPO possess  
48 antimicrobial activity similar to what found in mammals, where it could inhibit bacterial  
49 proliferation as constituent in ETs (Chi and Sun, 2016; Zhao et al., 2017; Gan et al.,  
50 2023).

51 The *MPO* gene has previously been cloned and the tissue distribution in some teleost  
52 has been described (Gan et al., 2023). However, MPO expression and content during  
53 flounder *Paralichthys olivaceus* (*PoMPO*) ontogeny have not yet been studied. Here,  
54 we studied the expression of *PoMPO* mRNA and protein at various stages during fish  
55 development and compared the fraction of MPO positive cells relative to other  
56 leucocytes from larvae to juvenile and adult stages. This study provided knowledge on  
57 early innate defense mechanisms in flounder, assessed by the occurrence of *PoMPO* -  
58 which is mainly expressed by neutrophils.

59

## 60 **Material and Methods**

### 61 **Sample collection and preparation**

62 Flounder larvae from 1 to 35 days post-hatch (dph), juveniles (~10 cm in length, ~75

63 dph) and adults (~30 cm, ~240 dph) were obtained from a farm located in Qingdao,  
64 Shandong province, China, and reared in recirculating seawater at 20 °C. The larvae  
65 were fed with *Artemia* until weaning and were switched to dry feed at approximately  
66 20 dph and sampled at 1, 4, 7, 10, 14, and 35 dph. The juvenile and adult fish were fed  
67 daily with a commercial dry feed pellet. By clinical examination, the fish were assessed  
68 to be healthy. Before sampling, the fish were brought to euthanasia using 100 mg/L  
69 ethyl 3-aminobenzoate methanesulfonic acid (MS222, Sigma, St. Louis, MO, USA).  
70 Eighteen larvae were pooled at each time point and divided into three replicate groups  
71 for total RNA purification. For juveniles and adults, samples of liver, spleen, head  
72 kidney, gill, intestine, skin, and muscle were obtained from three fish. All samples were  
73 immediately frozen in liquid nitrogen until RNA isolation. These protocols for animal  
74 care and handling were approved by the Animal Care and Use Committee of Ocean  
75 University of China (Permit Number: 20180101).

#### 76 **Purification of total RNA and real-time quantitative PCR**

77 Total RNA was extracted from hatchlings or tissues (at late timepoints) from flounder  
78 by the Trizol method according to the manufacturer's protocol (Vazyme, Nanjing,  
79 China). The cDNA strand was synthesized by using Hiscript III RT SuperMix kit  
80 (Vazyme). The expression level of *PoMPO* mRNA was measured by using specific  
81 primers (forward primer: 5'-AGATCTGTCCCGATGAACGC-3' and reverse primer:  
82 5'-TTACAGCTATCACCCGAGCC-3'), 2 × Universal SYBR Green Fast qPCR Mix  
83 (Abclonal, Wuhan, China), and LightCycler® 480 II Real-Time System (Roche, Basel,  
84 Switzerland). The relative transcriptional levels of *PoMPO* were normalized against the

85 housekeeping gene 18S (forward primer: 5'-GGTCTGTGATGCCCTTAGATGTC-3'  
86 and reverse primer: 5'-AGTGGGGTTCAGCGGGTTAC-3'). All reactions were  
87 carried out in triplicate. The expression levels of *PoMPO* gene were analyzed using the  
88  $2^{-\Delta Ct}$  method with 18S serving as the internal control. Finally, the lowest expression  
89 level was used as the standard to calibrate the expression of other tissues.

#### 90 **Western blotting**

91 Hatchlings or tissues were lysed with RIPA Lysis Buffer Kit (Beyotime, Shanghai,  
92 China) containing a protease inhibitor. The protein concentration of the lysates was  
93 assessed by using the BCA kit (EpiZyme, Shanghai, China). The lysates (~20  $\mu$ g  
94 proteins) went through SDS-PAGE and electroblotted onto polyvinylidene fluoride  
95 membrane (Merck Millipore, Darmstadt, Germany). After blocking with BSA, the  
96 mouse anti-r*PoMPO* Abs ([Gan et al., 2023](#)) or rabbit anti-GAPDH Abs (Abclonal,  
97 Wuhan, China) was incubated with the membrane overnight at 4 °C. After washing three  
98 times, goat anti-mouse IgG-HRP or goat anti-rabbit IgG-HRP (Sigma, St. Louis, Mo,  
99 USA) was added according to standard protocol. Protein bands were visualized using a  
100 chemiluminescence detection instrument (Vilber, Ile-de-France, France).

#### 101 **Histological preparation**

102 Pre-metamorphic larva (14 dph, before eye migration, ~0.8 cm in length), and  
103 metamorphic climax larva (35 dph, right eye has migrated over the dorsal midline, ~1.2  
104 cm) were fixed overnight in Bouin's fixative (Phygene, Fujian, China) at room  
105 temperature. In the case of juveniles and adults, lymphoid tissues including head kidney,  
106 spleen, intestine, and gill were also sampled and fixed. All the fixed samples were

107 dehydrated in ethanol solutions and embedded in paraffin (Hushi, Shanghai, China).  
108 The paraffin blocks were sectioned at thickness of 5  $\mu\text{m}$ , and the sections of larvae were  
109 stained with hematoxylin-eosin (H&E) for morphological study.

#### 110 **Isolation of leukocytes from peritoneal cavity, peripheral blood and head kidney**

111 The leukocytes in the peritoneal cavity (PerCs), peripheral blood (PBLs) and head  
112 kidney (HKLs) of juveniles were isolated according to the previous report (Gan et al.,  
113 2023). For peritoneal cell isolation, the cells were harvested by lavaging peritoneal  
114 cavity with L-15 medium. The peripheral blood was drawn from the caudal vein and  
115 mixed with the anticoagulant (RPMI-1640 containing 20 IU  $\text{mL}^{-1}$  heparin, 0.1% w/v  
116  $\text{NaN}_3$ , and 1% w/v BSA) at a volume ratio of 1:2. The head kidney was cut into small  
117 pieces and grinded with adding RPMI-1640 (VivaCell, Shanghai, China). The solution  
118 was collected and filtered by a cell strainer to obtain a cell suspension. Then the  
119 leukocytes were isolated by Percoll (GE Healthcare, Uppsala, Sweden) density  
120 centrifugation, on a discontinuous density gradient (1.020/1.070  $\text{g mL}^{-1}$ ). All cells were  
121 subsequently resuspended in L-15 medium and adjusted to a concentration of  $1 \times 10^6$   
122 cells  $\text{mL}^{-1}$ . The isolated cells were processed for Wright-Giemsa staining, and then the  
123 images were taken using a microscope (Olympus, Tokyo, Japan).

#### 124 **Immunofluorescence staining**

125 The cells ( $1 \times 10^6$  cells  $\text{mL}^{-1}$ ) were seeded onto adhesion microscope slides (Citotest,  
126 Jiangsu, China) for 1 h, and then fixed with 4% paraformaldehyde (Solarbio, Beijing,  
127 China). The sections of flounder larvae and tissue were deparaffinized and rehydrated  
128 in graded series of ethanol. Antigen retrieval was performed at 95  $^{\circ}\text{C}$  in citrate antigen

129 retrieval solution (pH = 6.0, Beyotime, Shanghai, China) for 15 min to retrieve antigens.  
130 Endogenous peroxidase activity was quenched by incubation by a 1% H<sub>2</sub>O<sub>2</sub> in methanol  
131 (Hushi, Shanghai, China) solution for 20 min. The cells were permeabilized by 0.25%  
132 Triton X-100 (Solarbio, Beijing, China) in 5% BSA. Mouse anti-r*Po*MPO Abs, or anti-  
133 rTrx Abs ([Gan et al., 2023](#)) was used as the primary antibody onto the slides for  
134 overnight at 4 °C, followed by Alexa Fluor 649-conjugated goat anti-mouse IgG  
135 antibodies (Sigma, St. Louis, Mo, USA). Cells were counterstained with 2-(4-  
136 Amidinophenyl)-6-indolecarbamide dihydrochloride (DAPI, Thermo Scientific,  
137 Massachusetts, USA) and observed by a fluorescence microscopy (ZEISS, Oberkochen,  
138 Germany).

#### 139 **Flow cytometry**

140 The PerCs, HKLs and PBLs were fixed and permeabilized using BD Cytotfix/Cytoperm  
141 plus kit (BD Biosciences, San Diego, CA) to allow for intracellular examination of  
142 MPO by mouse anti-r*Po*MPO Abs. The cells were then incubated with Alexa Fluor 649-  
143 conjugated goat anti-mouse IgG secondary antibodies (Sigma, St. Louis, Mo, USA) for  
144 45 min at 37 °C in the dark. Mouse anti-rTrx Abs were used as negative controls. Flow  
145 cytometry was performed using FACSCalibur (BD Biosciences) flow cytometer with  
146 acquisition enabled by CellQuest Pro software.

#### 147 **Statistical analysis**

148 One-way analysis of variance (ANOVA) and Duncan's multiple comparisons were  
149 performed by using Statistical Product and Service Solution (SPSS) software (Version  
150 19.0; SPSS, IBM, BY, USA). For assessment of the results,  $P < 0.05$  was considered



151 statistically significant.

## 152 **Results**

### 153 **Ontogenic appearance of *PoMPO* mRNA and protein**

154 *PoMPO* mRNA levels at different time points post hatch, ranging from larvae to  
155 juvenile stages, were analyzed by real-time quantitative PCR (qPCR) (Fig. 1). At the  
156 larvae stage, the *PoMPO* gene was expressed in all samples. *PoMPO* gene expression  
157 was observed already on 1 dph and increased continuously to 14 dph ( $P < 0.05$  between  
158 each time point) (Fig. 1B). At the juvenile stage, the highest levels of *PoMPO* mRNA  
159 were observed in the head kidney, followed by the gill, spleen, intestine. The expression  
160 levels in the skin, muscle and liver were relatively low (Fig. 1D).

161 Western blotting revealed *PoMPO* protein presence in both larvae and juveniles.  
162 Consistent with the mRNA expression pattern, *PoMPO* was detected in homogenates  
163 from all sample time-points of larvae (Fig. 1A). For juveniles, the protein was found  
164 mainly in the head kidney and spleen, while no to minor content were found in gill,  
165 skin, muscle, and liver (Fig. 1C).

### 166 ***PoMPO*<sup>+</sup> cells during ontogeny**

167 To analyze the presence and distribution of *PoMPO*<sup>+</sup> cells during different ontogenic  
168 stages, the immunological organs of the pre-metamorphic larvae, metamorphic climax  
169 larvae, juvenile, and adult individuals were investigated by immunofluorescence. At the  
170 stage just before metamorphosis, the kidney developed into an adult-like organ. The  
171 kidney fused along the ventral part of peritoneal cavity, with a visible head kidney and  
172 trunk kidney (Fig. 2A, B). The head kidney is an important immune organ in teleost,

173 thus some *PoMPO*<sup>+</sup> cells were found scattered in the kidney (Fig. 2B, C). The kidney  
174 became larger in the metamorphic climax larvae and *PoMPO*<sup>+</sup> cells were observed not  
175 only in the head kidney, but also along the renal part of the trunk kidney (Fig. 3A, B).  
176 However, *PoMPO*<sup>+</sup> cells were, at this stage, more numerous in the head kidney  
177 compared to trunk kidney (Fig. 3B, C). In juveniles and adults, head kidney seemed to  
178 be an important pool for *PoMPO*<sup>+</sup> cells (Fig. 4). The spleen of the flounder is a small  
179 spheric organ and increases in size as the fish grows (Fig. 2A, Fig. 3A). In the pre-  
180 metamorphic larvae, only a few *PoMPO*<sup>+</sup> cells were found in the spleen (Fig. 2D).  
181 During the development into metamorphic climax larva, the number of *PoMPO*<sup>+</sup> cells  
182 increased and the cells were observed scattered throughout the spleen (Fig. 3D). In  
183 juvenile and adult individuals, a relatively high number of *PoMPO*<sup>+</sup> cells were found  
184 in the spleen (Fig. 4).

185 The gills of flounder are bilaterally situated on either side of the pharynx, composed of  
186 gill arches and primary lamellae (Fig. 2A, Fig. 3A). In the pre-metamorphic larva,  
187 though the differentiation of gills seemed to be inconspicuous, a few *PoMPO*<sup>+</sup> cells  
188 were detected. At the metamorphic climax larvae stage, *PoMPO*<sup>+</sup> cells were detected in  
189 the primary gill lamellae and in the gill filaments along blood vessels (Fig. 2E, Fig. 3E).  
190 As the flounder grew older, the distribution and number of *PoMPO*<sup>+</sup> cells appeared to  
191 be similar compared to juvenile and adult stages (Fig. 4). In the flounder, the intestine  
192 is composed of four layers, namely lamina epithelialis, lamina propria, lamina  
193 muscularis and serosa. In the pre-metamorphic larvae, this layered structure of the  
194 intestine was not clearly observable compared to the metamorphic climax stage. In the

195 metamorphic climax larvae, *PoMPO*<sup>+</sup> cells were dispersed predominantly in the lamina  
196 epithelialis (Fig. 2F, Fig. 3F). As the flounder grew older, the *PoMPO*<sup>+</sup> cells were  
197 mainly located in the lamina propria at juvenile and adult stages (Fig. 4). No  
198 fluorescence was observed in the negative controls from the selected organs (Fig. S2A-  
199 D).

#### 200 **Presence and distribution of *PoMPO*<sup>+</sup> cells in juvenile and adult flounder**

201 The presence and proportion of *PoMPO*<sup>+</sup> cells from juveniles were assessed in total  
202 leucocytes extracted from the peritoneal cavity, head kidney, and peripheral blood (Fig.  
203 5). The results of Giemsa staining showed that the PerCs and HKLs contained many  
204 granulocytes with the nuclei located on the cellular side and relatively faintly stained  
205 cytoplasm, while the PBLs mainly contained lymphoid cells possessing a large nucleus  
206 with less cytoplasm (Fig. S1). Indirect immunofluorescence assay demonstrated that  
207 *PoMPO* was dispersed throughout the entire cytoplasm. The nuclei of *MPO*<sup>+</sup> cells were  
208 darker compared to other leucocyte-like cells (Fig. 4, Fig. 5). No fluorescence was  
209 observed in the negative controls (Fig. S2E). Flow cytometry revealed that the  
210 proportion of *PoMPO*<sup>+</sup> cells to leukocytes in the peritoneal cavity, head kidney, and  
211 peripheral blood of juvenile flounders was 18.3%, 34.8%, and 6.0%, respectively (Fig.  
212 5A-C).

#### 213 **Discussion**

214 Flatfish possess metamorphosis during its development, which is a gradual process of  
215 maturation of larval morphology and anatomy into a juvenile morphology.  
216 Morphological assessment is often the most used criterium to determine the early stages

Kommentert [RD1]: What do you mean by «cellular side»?

217 of development where right eye movement and the disappearance of coronal fins are  
218 the key characteristics (Falk-Petersen, 2005; Miwa and Inui, 1987). As one of the first  
219 defensive response against invading pathogens, neutrophils are rapidly recruited to  
220 infection and inflammation foci, where they recognize, phagocytose, inactivate  
221 microorganisms, perform immunomodulatory effects, and may act as antigen-  
222 presenting accessory cells involved in the induction stage of adaptive immunity (Gan  
223 et al., 2023; Arnhold, 2020; Marcinkiewicz and Walczewska, 2020; Mantovani et al.,  
224 2011). Determining the quantity and density of MPO<sup>+</sup> cells in fish immune system  
225 during ontogeny is helpful to assess the maturity of immune organs and possibly to  
226 track the onset of functional innate mechanisms. The knowledge can be exploited  
227 further to find the right time for innate immunity training and vaccination.

228 MPO is a member of the heme peroxidase-cyclooxygenase superfamily, which could  
229 kill e.g., trapped bacteria by virtue of extracellular traps, and is involved in other  
230 functions neutrophils, such as neutrophil trafficking, activation, phagocytosis, and  
231 lifespan (Rizo-Téllez et al., 2022). In mammals, MPO is correlated well with tissue  
232 neutrophil content, can be used as a marker to assess neutrophil infiltration in the tissue  
233 (Pulli et al., 2013). In turbot, potassium iodide and oxidized pyronine Y (KI-PyY)  
234 stained MPO<sup>+</sup> cells exhibited characteristics of neutrophil morphology (Chi et al., 2017).  
235 In one of our previous studies *PoMPO* was found to mainly exist in granulocytes and  
236 macrophages which indicated that these two types of cells may have some function that  
237 share, such mediating microbial killing. *PoMPO* exists in ET scaffold and is involved  
238 in the antibacterial effect of ETs (Gan et al., 2023). In humans, neutrophils first appear

239 in bone marrow by 10-11 weeks of gestation, and then mature neutrophils are released  
240 from the bone marrow about three weeks later (Leiding, 2017). In foals, MPO gene  
241 expression is present in newborns and the expression increases with age, reaching  
242 highest levels at day 30 (Ghaeli et al., 2022). Opossum are considered as a model  
243 species for investigations regarding the evolution of the mammalian immune system.  
244 They are born with a low number of neutrophils, but in a few weeks later the neutrophils  
245 become the predominant leukocyte (Fingerhut et al., 2020). In zebrafish, the earliest  
246 MPO expression has been detected in cells of the intermediate cell mass right before  
247 one-day post-fertilization (18 hours post fertilization) (Shen et al., 2013). In this study,  
248 *PoMPO* transcripts and protein were detected already at 1 dph and were subsequently  
249 found widely expressed in major immune organs as the fish grew to a juvenile stage,  
250 especially from pre-metamorphic larvae to metamorphic climax larvae. ~~It can be  
251 speculated that *PoMPO* is involved in processes related to organ e.g., development, and  
252 imply the functional enhancement in responsiveness to antigenic stimuli.~~ The similarity  
253 with respect to ontogenic development in fish compared to higher vertebrate animals  
254 may reflect a conserved evolutionary function of neutrophils (Fingerhut et al., 2020;  
255 Buchmann, 2022; Hauser et al., 2023).

256 In teleost, the head kidney is regarded to be the bone marrow equivalent in vertebrates,  
257 being hemopoietic (Rauta et al., 2012; Bjørgen and Koppang, 2022). The spleen also  
258 plays a role in hematopoiesis, antigen trapping, and antibody production (Uribe et al.,  
259 2011). The gills and intestine are both tissues with continuous exposure to seawater and  
260 possibly pathogens. As such, a wide distribution of leukocytes, including T cells, B cells,

Komment [RD2]: I think you should remove this speculation.

261 plasma cells, macrophages and granulocytes is vital (Salinas et al., 2011) The  
262 maturation of fish immune system occurs, depending on the species under study, in a  
263 few weeks after hatching, and it has been shown that mandarin fish may require at least  
264 3 weeks after to be able to mount a more advanced immune response involving adaptive  
265 immunity (Grøntvedt and Espelid, 2003; Tian et al., 2009). In some teleost, such as in  
266 the Atlantic halibut, the immune organs mature both morphologically and functionally  
267 in the period after the start of exogenous feeding, and at 94 dph they possess IgM  
268 positive cells and secreted IgM (Patel et al., 2009). The tissue distribution of *PoMPO*  
269 mRNA and protein in juvenile flounder at day 75 was comparable with the expression  
270 pattern in adult fish, where *PoMPO* previously has been shown to be highly expressed  
271 in head kidney and gills, followed by spleen and intestine (Gan et al., 2023). These  
272 findings suggest that 75 days after hatch, the flounder has reached a mature state –  
273 although not proven functionally. Supportively, the highest proportion of *PoMPO*<sup>+</sup> cells  
274 relative to leukocytes in the head kidney of flounder juvenile stage was similar to the  
275 adult, where *PoMPO*<sup>+</sup> cells have previously been shown to account for approximately  
276 42% in head kidney leukocytes, which strongly indicates that the head kidney recruits  
277 neutrophils (Gan et al., 2023). However, during development, *PoMPO*<sup>+</sup> cells may likely  
278 follow the peripheral blood circulation system to patrol and settle in other organs such  
279 as heart, liver, and skin ~~may also play a role in immune or inflammatory responses.~~  
280 A major difference between teleost and mammals relates to the relative numbers of  
281 neutrophils in circulation. In humans, neutrophils make up 40% - 70% of leukocyte in  
282 circulation, compared to fish (approx. 5%) (40%-70%). The kidney of teleost has been

283 shown to house prominent neutrophilic populations (Havixbeck et al., 2015). In our  
284 study, the head kidney of flounder was found to contain significant neutrophilic  
285 populations compared to peritoneal cavity and blood. This suggests that the neutrophil  
286 hematopoiesis occurs in head kidney which also serve as a pool of mature neutrophils  
287 in bony fish a, which can traffic to more distant site upon microbial infection or  
288 inflammation.

289 In conclusion, the ontogenic distribution of myeloperoxidase in flounder were analyzed  
290 by using gene expression in combination with immunolabelling methods. These  
291 methods provided evidence for the ontogenic development of MPO positive cells, thus  
292 neutrophils, in flounder. These findings deepens our understanding of the onset and  
293 development of the immune system in teleost fish and may provide means to increase  
294 the survival of flounder larvae using e.g., immunostimulants targeting receptors specific  
295 for neutrophils.

296

#### 297 **Data availability**

298 Data will be made available on request.

299

#### 300 **Ethics Statement**

301 The animal study was reviewed and approved by the protocols for animal care and  
302 handling were approved by the Animal Care and Use Committee of Ocean University  
303 of China (Permit Number: 20180101).

304

305 **Author contribution**

306 Q.G., H.C., and R.A.D. were associated with the conception of the study. Q.G., H.C.,  
307 C.L., and L.Z. performed the experimental and statistical analyses, and wrote the  
308 original draft. R.A.D. edited the manuscript to the final version. H.C., R.A.D., J.X.,  
309 X.T., X.S., and W.Z. provided the funding. All authors read and approved the final  
310 version of the manuscript.

311

312 **Funding**

313 This research was funded by grants from the National Key Research and Development  
314 Program of China (2023YFD2400703), the Fundamental Research Funds for the  
315 Central Universities (No. 202212012), the National Natural Science Foundation of  
316 China (32373160 & 31872594), and the Young Talent Program of Ocean University of  
317 China (No. 2022010042). The Research Council of Norway (grant no. 301401 and  
318 32519) is acknowledged.

319 **Declaration of competing interest**

320 The authors declare that the research was conducted in the absence of any commercial  
321 or financial relationships that could be construed as a potential conflict of interest.

322 **Reference**

323 Austin, B., 2006. The bacterial microflora of fish, revised. *Sci. World J.* 6, 931-945.  
324 <https://doi.org/10.1100/tsw.2006.181>  
325 Arnhold, J., 2020. The dual role of myeloperoxidase in immune response. *Int. J. Mol.*  
326 *Sci.* 21, 8057. <https://doi.org/10.3390/ijms21218057>.



327 Aratani, Y., 2018. Myeloperoxidase: Its role for host defense, inflammation, and  
328 neutrophil function. Arch. Biochem. Biophys. 640, 47-52.  
329 <https://doi.org/10.1016/j.abb.2018.01.004>.

330 Bergh, Ø., 2000. Bacterial pathogens associated with early life stages of marine fish  
331 Microbial Biosystems: New Frontiers. Proceedings of the 8th International  
332 Symposium on Microbial Ecology. Halifax: Atlantic Canada Society for Microbial  
333 Ecology. 2000, 221-228.

334 Buchmann, K., 2022. Neutrophils and aquatic pathogens. Parasite Immunol. 44, e12915.  
335 <https://doi.org/10.1111/pim.12915>.

336 Bjørgen, H., and Koppang, E.O., 2021. Anatomy of teleost fish immune structures and  
337 organs. Immunogenetics. 73, 53-63. [https://doi.org/10.1007/s00251-020-](https://doi.org/10.1007/s00251-020-01196-0)  
338 [01196-0](https://doi.org/10.1007/s00251-020-01196-0).

339 Campoverde, C., Andree, K.B., Milne, D.J., Estévez, A., Gisbert, E., Carella, F., 2019.  
340 Ontogeny of lymphoid organs and mucosal associated lymphoid tissues in  
341 meagre (*Argyrosomus regius*). Fish Shellfish Immunol. 84, 509–520.  
342 <https://doi.org/10.1016/j.fsi.2018.09.033>.

343 Chi, H., Sun, L., 2016. Neutrophils of *Scophthalmus maximus* produce extracellular  
344 traps that capture bacteria and inhibit bacterial infection. Dev Comp Immunol.  
345 56,7-12. <https://doi.org/10.1016/j.dci.2015.11.005>

346 Chi, H., Wen, L.L., Sui, Z.H., Sun, Q.L., Sun, L., 2017. Cytochemical identification  
347 of turbot myeloperoxidase-positive granulocytes by potassium iodide and  
348 oxidized pyronine Y staining. Tissue Cell. 49, 751-755.

349 <https://doi.org/10.1016/j.tice.2017.10.008>.

350 Dalum, A.S., Kraus, A., Khan, S., Davydova, E., Rigaudeau, D., Bjørgen, H., López-  
351 Porras, A., Griffiths, G., Wiegertjes, G.F., Koppang, E.O., Salinas, I., Boudinot,  
352 P., Rességuier, J., 2021. High-Resolution, 3D Imaging of the Zebrafish Gill-  
353 Associated Lymphoid Tissue (GIALT) Reveals a Novel Lymphoid Structure,  
354 the Amphibranchial Lymphoid Tissue. *Front Immunol.* 12, 769901.  
355 <https://doi.org/10.3389/fimmu.2021.769901>.

356 Ellis, A.E., 1999. Immunity to bacteria in fish. *Fish Shellfish Immunol.* 9, 291-308.  
357 <https://doi.org/10.1006/fsim.1998.0192>.

358 Falk-Petersen, I. B., 2005. Comparative organ differentiation during early life stages of  
359 marine fish. *Fish Shellfish Immunol.* 19, 397-412.  
360 <https://doi.org/10.1016/j.fsi.2005.03.006>.

361 Fingerhut, L., Dolz, G., and de Buhr, N., 2020. What is the evolutionary fingerprint in  
362 neutrophil granulocytes?. *Int. J. Mol. Sci.* 21, 4523. [https://doi.org/](https://doi.org/10.3390/ijms21124523)  
363 [10.3390/ijms21124523](https://doi.org/10.3390/ijms21124523)

364 Gasteiger, G., D'Osualdo, A., Schubert, D.A., Weber, A., Bruscia, E.M., Hartl, D., 2016.  
365 Cellular Innate Immunity: An Old Game with New Players. *J. Innate Immun.* 9,  
366 111-125. <https://doi.org/10.1159/000453397>.

367 Gan, Q.J., Chi, H., Dalmo, R.A., Meng, X.H., Tang, X.Q., Xing, J., Sheng, X.Z., Zhan,  
368 W.B., 2023. Characterization of myeloperoxidase and its contribution to  
369 antimicrobial effect on extracellular traps in flounder (*Paralichthys olivaceus*).  
370 *Front Immunol.* 14, 1124813. <https://doi.org/10.3389/fimmu.2023.1124813>.

371 Ghaeli, T., Karimi, B., Kojouri, G.A., Dehkordi, R.R, Ahadi, A.M., 2022. The Influence  
372 of Age and Gender on the Serum XOR Activity, Leukocyte Gene Expression of  
373 XOR and MPO, and Biochemical Parameters in Newborn Foals. *J Equine Vet*  
374 *Sci.* 119, 104134. <https://doi.org/10.1016/j.jevs.2022.104134>.

375 Grøntvedt, R.N., Espelid, S., 2003. Immunoglobulin producing cells in the spotted  
376 wolffish (*Anarhichas minor* Olafsen): localization in adults and during juvenile  
377 development. *Dev. Comp. Immunol.* 27, 569-578.  
378 [https://doi.org/10.1016/S0145-305X\(03\)00028-4](https://doi.org/10.1016/S0145-305X(03)00028-4).

379 Hirayama, D., Iida, T., Nakase, H., 2017. The Phagocytic Function of Macrophage-  
380 Enforcing Innate Immunity and Tissue Homeostasis. *Int. J. Mol. Sci.* 19, 92.  
381 <https://doi.org/10.3390/ijms19010092>

382 Hauser, K.A., Garvey, C.N., Popovic, M., Grayfer, L., 2023. Biology of amphibian  
383 granulocytes - From evolutionary pressures to functional consequences. *Dev*  
384 *Comp Immunol.*, 140, 104623. <https://doi.org/10.1016/j.dci.2022.104623>.

385 Havixbeck, J.J., Barreda, D.R., 2015. Neutrophil Development, Migration, and  
386 Function in Teleost Fish. *Biology.*, 4, 715-734.  
387 <https://doi.org/10.3390/biology4040715>

388 Lee, M., Lee, S. Y., Bae, Y. S., 2022. Emerging roles of neutrophils in immune  
389 homeostasis. *BMB Rep.*, 55, 473–480.  
390 <https://doi.org/10.5483/BMBRep.2022.55.10.115>

391 Liang, C.C., Sheng, X.Z., Tang, X.Q., Xing, J., Chi, H., Zhan, W.B, 2022. Structural  
392 characteristics and mucosal immune response of the interbranchial lymphoid

393 tissue in the gills of flounder (*Paralichthys olivaceus*). *Fish Shellfish Immunol.*  
394 123, 388-398. <https://doi.org/10.1016/j.fsi.2022.03.022>.

395 Leiding, J. W., 2017. Neutrophil evolution and their diseases in humans. *Front.*  
396 *Immunol.* 8, 1009. <https://doi.org/10.3389/fimmu.2017.01009>.

397 Martin, S.A.M., Król, E., 2017. Nutrigenomics and immune function in fish: new  
398 insights from omics technologies. *Dev Comp Immunol.* 75, 86-98.  
399 <https://doi.org/10.1016/j.dci.2017.02.024>.

400 Malech, H.L., DeLeo, F.R., Quinn, M.T., 2020. The Role of Neutrophils in the Immune  
401 System: An Overview. *Methods in molecular biology (Clifton, N.J.)*, 2087, 3–10.  
402 [https://doi.org/10.1007/978-1-0716-0154-9\\_1](https://doi.org/10.1007/978-1-0716-0154-9_1).

403 Morales-Primo, A.U., Becker, I., Zamora-Chimal, J., 2022. Neutrophil extracellular  
404 trap-associated molecules: a review on their immunophysiological and  
405 inflammatory roles. *Int. Rev. Immunol.* 41, 253-274. <https://doi.org/10.1080/08830185.2021.1921174>.

407 Miwa, S., Inui, Y., 1987. Histological changes in the pituitary-thyroid axis during  
408 spontaneous and artificially-induced metamorphosis of larvae of the flounder  
409 *Paralichthys olivaceus*. *Cell Tissue Res.* 249, 117–123.  
410 <https://doi.org/10.1007/BF00215425>.

411 Marcinkiewicz, J., Walczewska, M., 2020. Neutrophils as sentinel cells of the immune  
412 system: a role of the MPO-halide-system in innate and adaptive immunity. *Curr.*  
413 *Med. Chem.* 27, 2840-2851.  
414 <https://doi.org/10.2174/0929867326666190819123300>.

415 Mantovani, A., Cassatella, M. A., Costantini, C., and Jaillon, S., 2011. Neutrophils in  
416 the activation and regulation of innate and adaptive immunity. *Nat Rev Immunol.*  
417 11,519-531. <https://doi.org/10.1038/nri3024>.

418 Odobasic, D., Kitching, A.R., Holdsworth, S.R., 2016. Neutrophil-mediated regulation  
419 of innate and adaptive immunity: the role of myeloperoxidase. *J. Immunol. Res.*  
420 2016, 2349817. <https://doi.org/10.1155/2016/2349817>.

421 Pulli, B., Ali, M., Forghani, R., Schob, S., Hsieh, K. L., Wojtkiewicz, G., Linnoila, J.  
422 J., Chen, J. W. 2013. Measuring myeloperoxidase activity in biological samples.  
423 *PloS One.* 8, e67976. <https://doi.org/10.1371/journal.pone.0067976>.

424 Patel, S., Sørhus, E., Fiksdal, I.U., Espedal, P.G., Bergh, Ø., Rødseth, O.M., Morton,  
425 H.C., Nerland, A.H., 2009. Ontogeny of lymphoid organs and development of  
426 IgM-bearing cells in Atlantic halibut (*Hippoglossus hippoglossus* L.). *Fish*  
427 *Shellfish Immunol.* 26, 385-395. <https://doi.org/10.1016/j.fsi.2008.11.018>.

428 Rojo-Cebreros, A.H., Ibarra-Castro, L., Martínez-Brown, J.M., 2018.  
429 Immunostimulation and trained immunity in marine fish larvae. *Fish Shellfish*  
430 *Immunol.* 80, 15-21. <https://doi.org/10.1016/j.fsi.2018.05.044>.

431 Rizo-Téllez, S.A., Sekheri, M., Filep, J.G., 2022. Myeloperoxidase: Regulation of  
432 Neutrophil Function and Target for Therapy. *Antioxidants* (Basel, Switzerland),  
433 11, 2302. <https://doi.org/10.3390/antiox11112302>.

434 Rauta, P.R., Nayak, B., and Das, S., 2012. Immune system and immune responses in  
435 fish and their role in comparative immunity study: a model for higher organisms.  
436 *Immunol. Lett.* 148, 23-33. <https://doi.org/10.1016/j.imlet.2012.08.003>.

437 Saurabh, S., Sahoo, P.K., 2008. Lysozyme: an important defence molecule of fish  
438 innate immune system. *Aquacult. Res.* 39, 223-239.  
439 <https://doi.org/10.1111/j.1365-2109.2007.01883.x>.

440 Sollberger, G., Tilley, D.O., Zychlinsky, A., 2018. Neutrophil Extracellular Traps: The  
441 Biology of Chromatin Externalization. *Dev Cell.* 44, 542-553.  
442 <https://doi.org/10.1016/j.devcel.2018.01.019>.

443 Shen, L.J., Cao, L.F., Chen, F.Y., Zhang, Y., Zhong, J.H., Zhong, H., 2013. Using  
444 modified whole-mount in situ hybridization to study mpo expression in  
445 zebrafish. *Exp Ther Med.* 5, 1043-1047. <https://doi.org/10.3892/etm.2013.947>.

446 Salinas, I., Zhang, Y.A., Sunyer, J.O., 2011. Mucosal immunoglobulins and B cells of  
447 teleost fish. *Dev. Comp. Immunol.* 35, 1346-1365. [https://doi.org/](https://doi.org/10.1016/j.dci.2011.11.009)  
448 [10.1016/j.dci.2011.11.009](https://doi.org/10.1016/j.dci.2011.11.009).

449 Tian, J.Y., Xie, H.X., Zhang, Y.A., Xu, Z., Yao, W.J., Nie, P., 2009. Ontogeny of IgM-  
450 producing cells in the mandarin fish *Siniperca chuatsi* identified by in situ  
451 hybridisation. *Vet. Immunol. Immunopathol.* 132, 146-152.  
452 <https://doi.org/10.1016/j.vetimm.2009.05.018>.

453 Uribe, C., Folch, H., Enríquez, R., Moran, G., 2011. Innate and adaptive immunity in  
454 teleost fish: a review. *Vet. Med.* 56, 486. [https://doi.org/10.17221/3294-](https://doi.org/10.17221/3294-VETMED)  
455 [VETMED](https://doi.org/10.17221/3294-VETMED).

456 Yúfera, M., Darias, M.J., 2007. The onset of exogenous feeding in marine fish  
457 larvae. *Aquaculture.* 268, 53-63.  
458 <https://doi.org/10.1016/j.aquaculture.2007.04.050>.

459 Zhao, M. L., Chi, H., Sun, L., 2017. Neutrophil Extracellular Traps of *Cynoglossus*  
460 *semilaevis*: Production Characteristics and Antibacterial Effect. Front  
461 Immunol. 8, 290. <https://doi.org/10.3389/fimmu.2017.00290>.  
462

463

464 **Figure legend**

465 **Fig. 1** Expression of *PoMPO* mRNA and protein during ontogeny. Lysates were  
466 harvested and subjected to western blotting analysis using by anti-r*PoMPO* and anti-  
467 GAPDH Abs was shown in larvae (A) and tissues of juvenile (C). The fold change of  
468 *PoMPO* mRNA in the larval flounder (B) and different organs of juvenile (D) by  
469 using qPCR analysis. The results were calculated by using relative expression method  
470 with 18S as the housekeeping gene. Different letters above the bar represent the  
471 statistical significance ( $P < 0.05$ ) compared to each other, and vertical bars  
472 represented the mean  $\pm$  SD, n = 3.

473 **Fig. 2** The H&E staining shows the morphological features (A) and indirect  
474 immunofluorescence assay indicates the positive signal of *PoMPO* in the tissues of pre-  
475 metamorphic larvae (B-F). A, bar = 500  $\mu$ m; B, bar = 200  $\mu$ m; C-F, bar = 50  $\mu$ m.

476 **Fig. 3** The H&E staining shows the morphological features (A) and indirect  
477 immunofluorescence assay indicats the positive signal of *PoMPO* in the tissues of  
478 metamorphic climax larvae (B-F). A, bar = 500  $\mu$ m; B, bar = 200  $\mu$ m; C-F, bar = 50  $\mu$ m.  
479 IEC: intestinal epithelial cell; LP: lamina propria.

480 **Fig. 4** *PoMPO*<sup>+</sup> cells detected by indirect immunofluorescence and flow cytometric  
481 analysis. Indirect immunofluorescence assay showed the positive signal of *PoMPO* in  
482 different tissues of juvenile and adult flounder. Bar = 50  $\mu$ m. IEC: intestinal epithelial  
483 cell; LP: lamina propria.

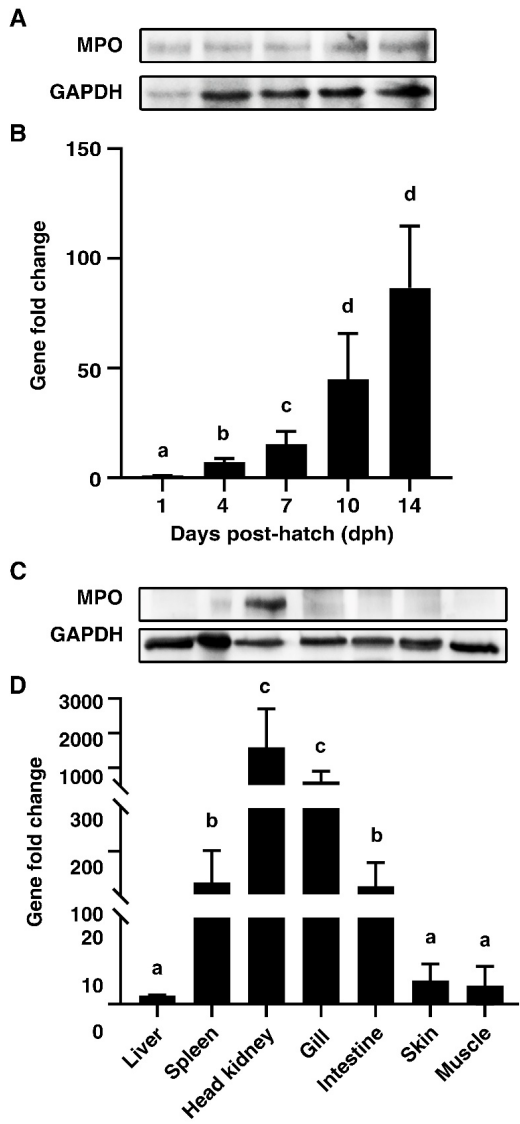


484 **Fig. 5** Indirect immunofluorescence assay and flow cytometric analysis of *PoMPO*<sup>+</sup>  
485 cells in PerCs (A), HKLs (B) and PBLs (C). The scatter plot showed the gate of FSC  
486 area (FSC-A)/SSC area (SSC-A) of juvenile flounder. Fluorescence histogram showed  
487 the ratio of *PoMPO*<sup>+</sup> cells in gated leukocytes. The representative results from three  
488 different individuals.

489 **Fig. S1** The Giemsa stain analysis of PerCs, HKLs and PBLs in flounder. LY:  
490 lymphocyte; MA: macrophages; GR: granulocytes. Bar = 10  $\mu$ m.

491 **Fig. S2** The indirect immunofluorescence assay using mouse anti-rTrx Abs as the first  
492 antibody for negative controls to the positive signal of *PoMPO* in the tissues of pre-  
493 metamorphic larvae (A), metamorphic climax larvae (B), juvenile (C) and adult  
494 flounder (D), the cells in the peritoneal cavity, head kidney and peripheral blood (E).  
495 Blue indicates the nuclei stained by DAPI. Red shows the positive signal or background  
496 noise.

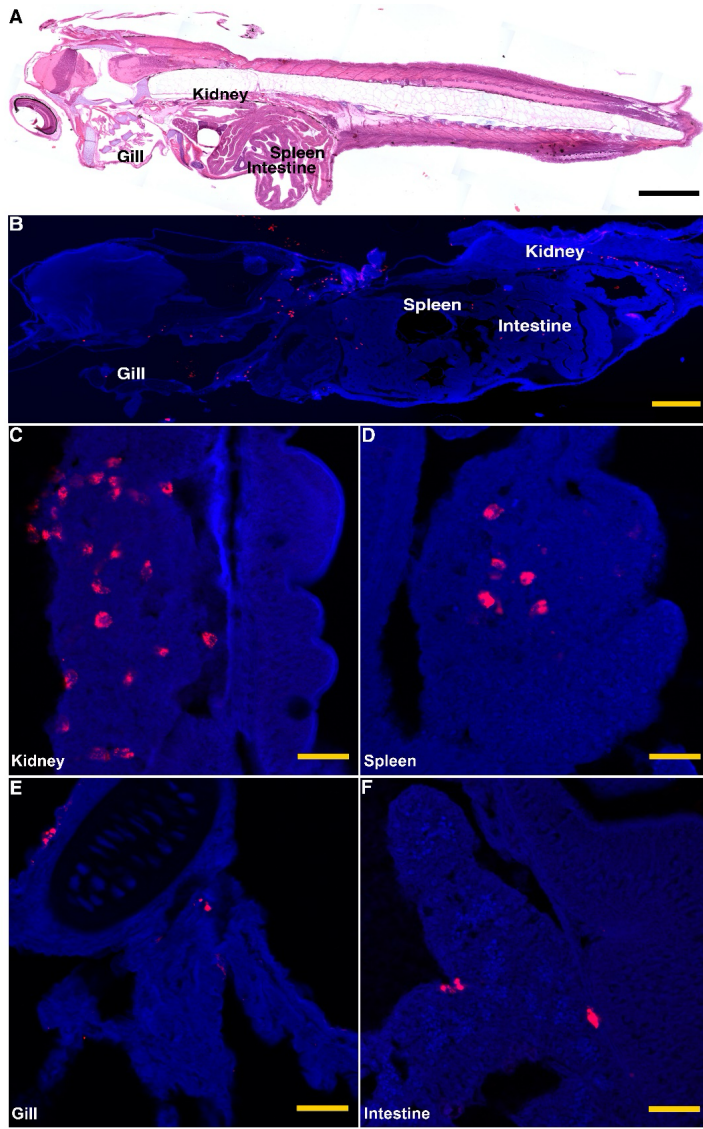
497 Fig. 1



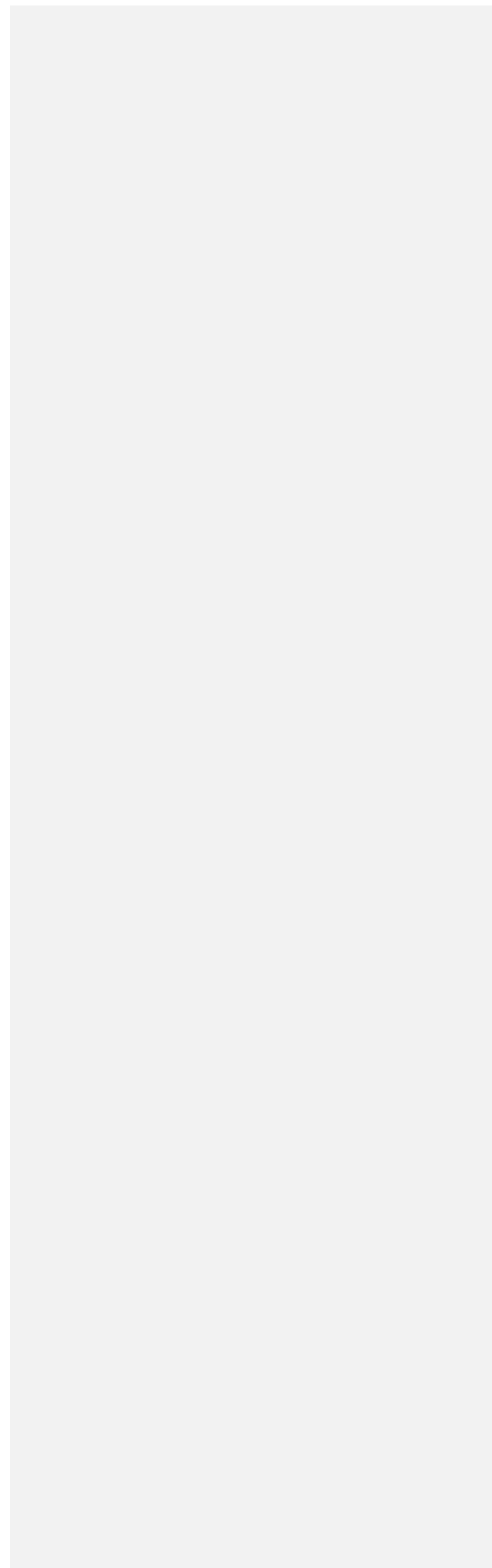
498

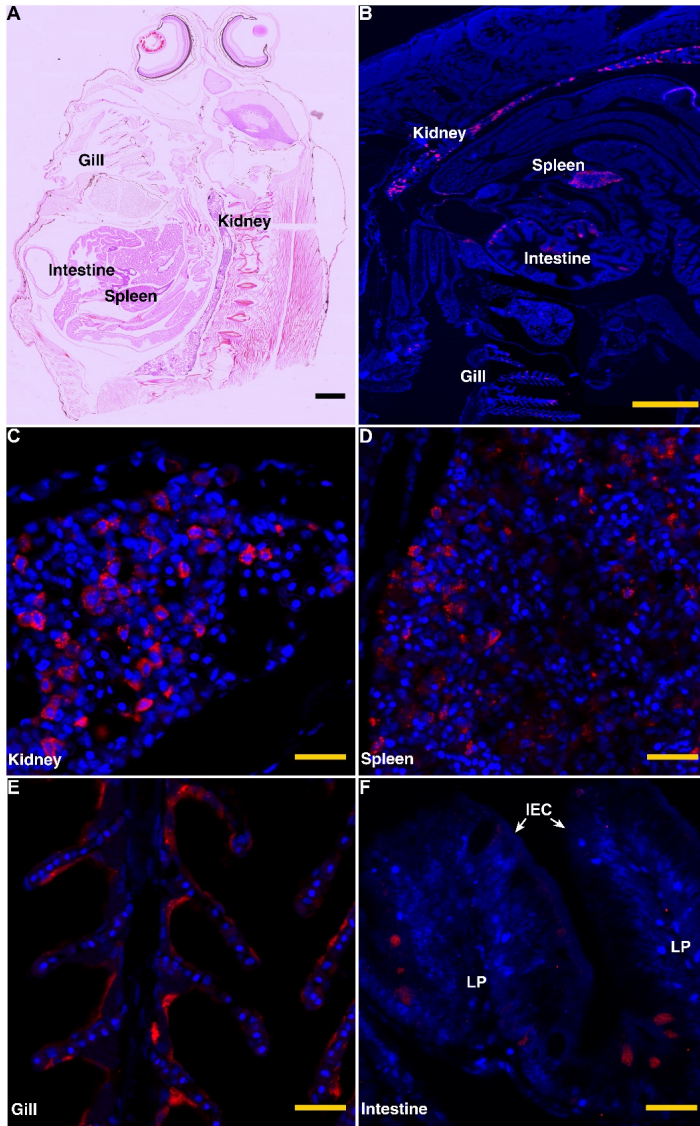
499

500 Fig. 2

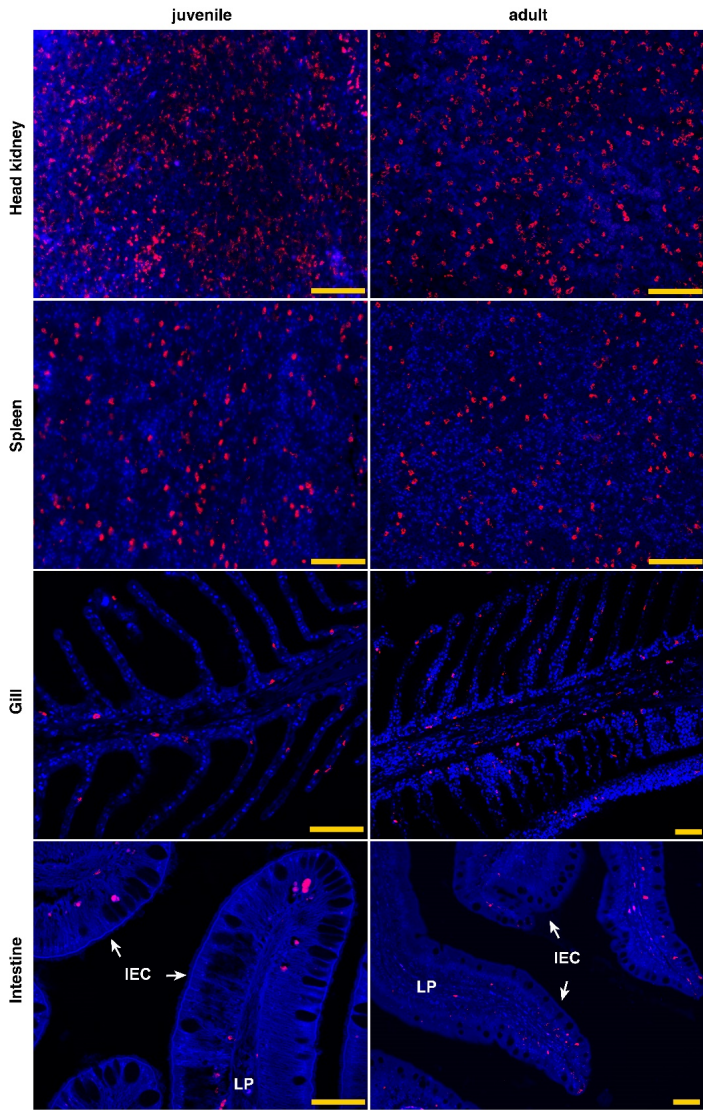


501  
502

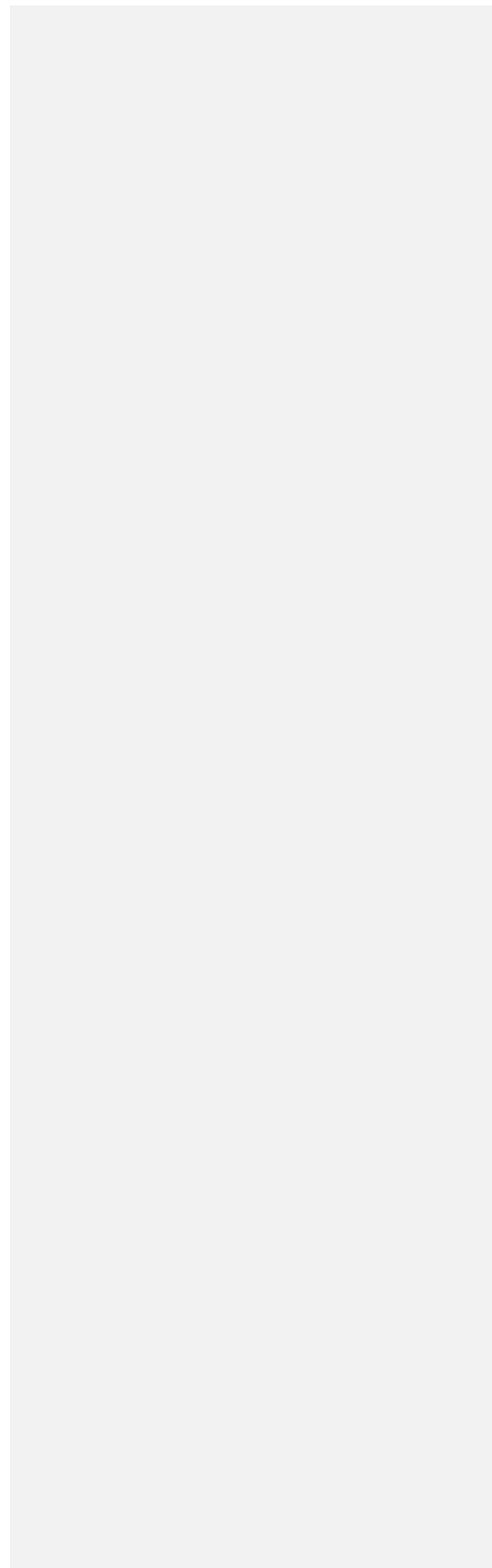


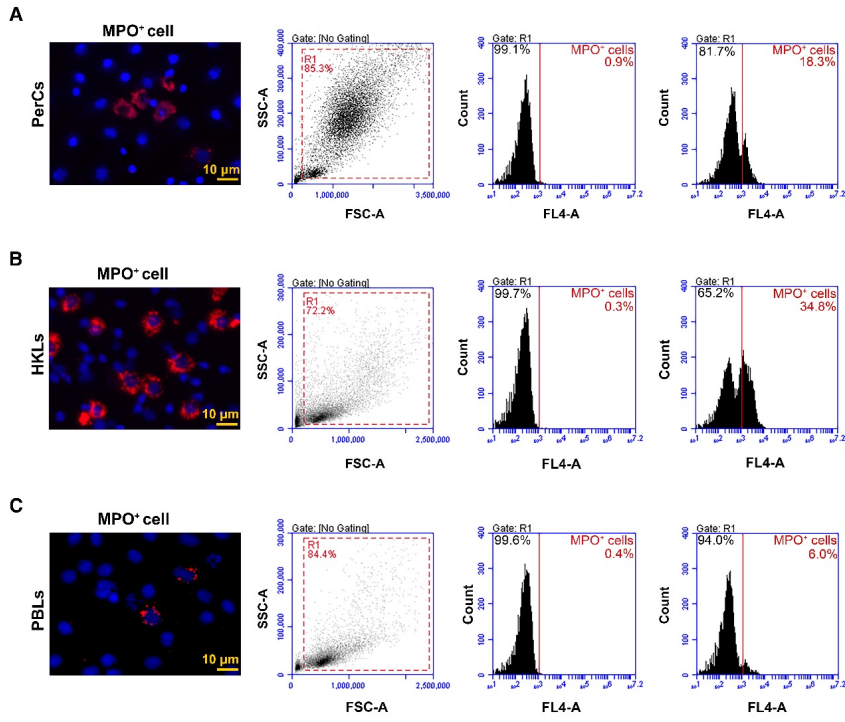


506 Fig. 4



507  
508

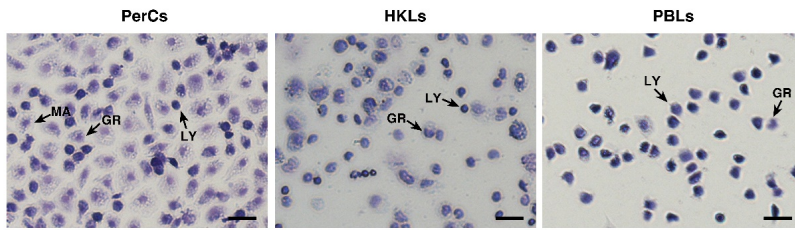




510

511

512 Fig. S1



513  
514

